ACS Catalysis

pubs.acs.org/acscatalysis Letter

Operando EPR Study of Radical Formation in Anion-Exchange Membrane Fuel Cells

Szymon Wierzbicki, John C. Douglin, Ramesh K. Singh, Dario R. Dekel,* and Krzysztof Kruczała*

Cite This: ACS Catal. 2023, 13, 2744−2750 Read Online

ACCESS | Metrics & More | Article Recommendations | Supporting Information

ABSTRACT: The alkaline operating environment of anion-exchange membrane (AEM) fuel cells (AEMFCs) makes it possible to employ a wide variety of catalysts, including platinum group metals (PGMs) as well as PGM-free materials. However, little is understood about radical formation during AEMFC operation with different catalysts and their implications. In this investigation, we utilized spin-trapping and electron-paramagnetic resonance measurements to measure and identify the radicals produced on selected PGM and PGM-free oxygen-reduction reaction catalysts. To the best of our knowledge, this is an original study exploring radical formation on different classes of catalysts in operando AEMFCs. This work highlights an unexplored radical degradation mechanism in AEMFCs and calls for innovative strategies in designing radical attack-resistant AEMs.

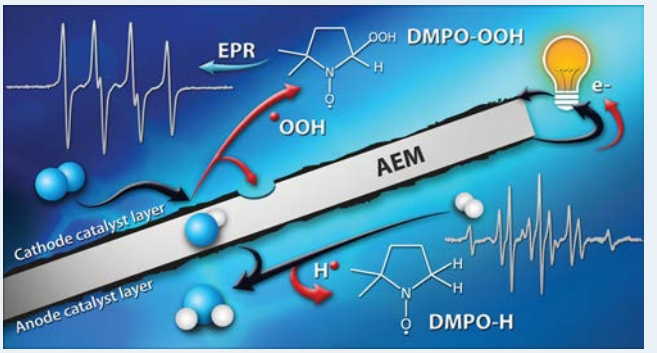

KEYWORDS: *Anion-Exchange Membrane Fuel Cells (AEMFC), EPR spin trapping, radical reactions, radical-induced degradation, oxygen reduction reaction (ORR)*

INTRODUCTION

Anion-exchange membrane fuel cells (AEMFCs) are regarded as a promising fuel cell technology because of their significant potential to replace the current expensive proton-exchange membrane fuel cell (PEMFC).[1−3] Recently, AEMFCs achieved remarkable power densities[4−7] with high voltage efficiencies, which makes the technology a serious contender for matured PEMFCs. Additionally, AEMFCs provide the opportunity to incorporate platinum group metal (PGM)-free[8−15] catalysts into the electrodes, as well as a greater variety of low-cost polymers for use as membranes.[1] In spite of these benefits, major challenges still need to be addressed before this technology can be utilized in practical applications. The most pressing is the long-term stability of the AEMFC[3,14,16] and the use of completely PGM-free electrodes.[14,15,17]

In a recent review of the various aspects of AEMFC durability, Mustain et al. summarized that further comprehension of the anion-exchange membrane (AEM), electrode materials, anion-exchange ionomer, catalyst layer optimization, and water management is crucial in order to meet the durability target set by the U.S. DOE.[14] However, they have not discussed the mechanism of radical formation and how it affects the AEMFCs' durability. Very recently, we have shown for the first time the formation and presence of stable radicals during operando AEMFCs.[18] During the operation of Pt-based AEMFCs, we have reported 5,5-dimethyl-1-pyrroline N-oxide (DMPO)-OOH and DMPO−OH radicals on the cathode electrode and DMPO-H on the anode electrode. Therefore, evaluating the potential of PGM and in particular PGM-free electrodes to generate radicals during the operation of AEMFCs has crucial importance.

In this study, we report for the first time on the formation of radicals during the operation of AEMFCs based on various selected PGM and PGM-free catalysts by operando electron paramagnetic resonance (EPR). We focus on the cathode electrode where the electrochemical oxygen reduction reaction (ORR) takes place and reactive oxygen species may be formed. We specifically employed Pd, Ag, PdAg, and $(MnCo)_3O_4$ as cathode catalysts to investigate the potential of oxygen radicals formed in different classes of catalysts. These catalysts are chosen as they have relatively high activities as cathodes in AEMFCs,[11−13,19−21] and they are significantly different.

EXPERIMENTAL SECTION

CCMs were prepared for use in operando EPR measurements with Pd that was obtained from Sigma-Aldrich, Ag from Nanogap, and PdAg purchased from NanoShel. Also, the

Received: November 28, 2022
Revised: January 31, 2023
Published: February 7, 2023

https://doi.org/10.1021/acscatal.2c05843
ACS Catal. 2023, 13, 2744−2750

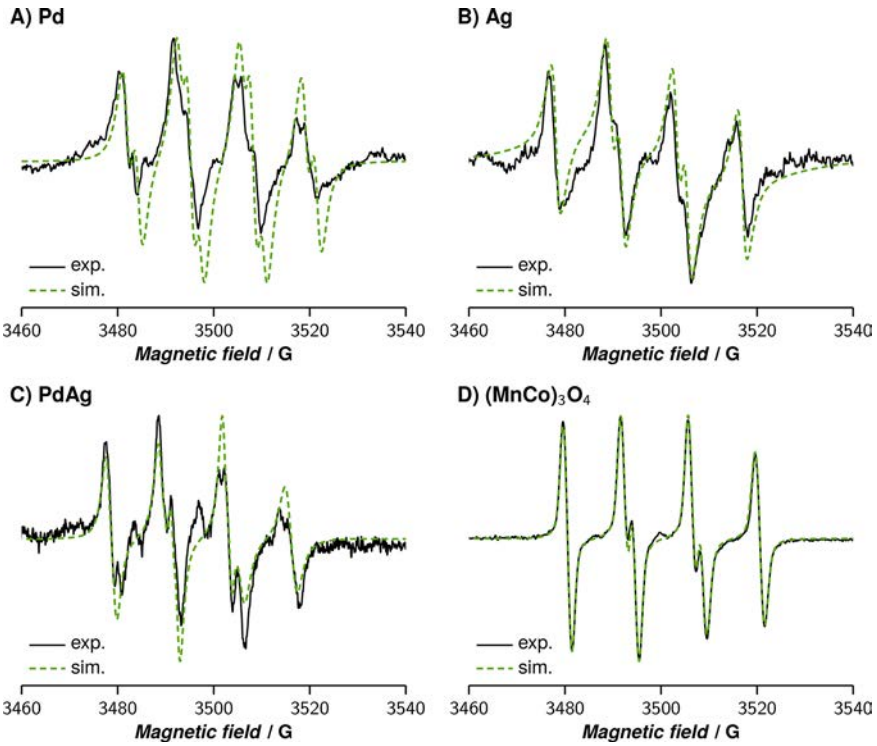

Figure 1. Experimental (black solid line) and simulated (green dashed line) EPR spectra of DMPO-OOH adducts formed during the operation of AEMFCs using various cathode catalysts: Pd (A), Ag (B), PdAg (C), and $(MnCo)_3O_4$ (D).

$(MnCo)_3O_4$ spinel catalyst was synthesized as described elsewhere.[22] Further details are given in the Materials i (p 2) and Experimental Methods i and ii (Figure S1, p 3) sections as well as active area loadings of the CCMs in Table S1 of the Supporting Information (SI).

EPR measurements were carried out at room temperature using a Bruker ELEXYS E500 spectrometer, equipped with a super-high-sensitivity Bruker ER 4122 SHQE cavity operating at 9.7 GHz and 100 kHz magnetic field modulation. EPR spectra were simulated using SimEPR32 software.[23] Before commencing the *operando* experiments, a pure liquid DMPO spin trap (0.5 μL, Enzo) was deposited on the cathode side using an automatic micropipette. The CCMs (see Table S1) were then placed inside a fuel cell (5 mm in diameter),[18,24] with two platinum wires used as current collectors. The cell was run under closed circuit voltage (CCV) conditions, connected serially to the Velleman DVM898 digital voltmeter with an internal resistance > 100 MΩ, used for monitoring the cell voltage, which varied between 0.2 and 0.5 V depending on the exact anode/cathode catalyst combination. The cell was fed with 2−5 sccm/min of pure hydrogen and oxygen (AirProducts, N5.0).

To gain an insight into the ORR performance of the investigated catalysts, the rotating ring-disk electrode (RRDE) technique and AEMFC testing methods were used. For the RRDE tests, catalytic inks were prepared by sonicating catalysts with 2-propanol and Nafion solution, followed by dropcasting the inks onto 5 mm glassy carbon (GC) disc electrode. For the AEMFC tests, cathode catalyst slurries were deposited directly onto gas diffusion layers to prepare gas diffusion electrodes (GDEs), which were then combined with PtRu-based anode GDEs and FAA-3-5-rf AEMs to produce membrane-electrode assemblies (MEAs). The tests were carried out with H_2−O_2 feeding gases. Further details on these tests are given in the SI (section Experimental Methods v and vi, Figures S2−S6, and Tables S2 and S3).

RESULTS AND DISCUSSION

The X-ray powder diffraction investigation of the $(MnCo)_3O_4$ sample confirms the formation of a nanosized oxide of the spinel structure, with a size of 6.2 nm as calculated from the Scherrer formula (Figure S1).[25] The onset potential, E_{onset}, of the spinel catalyst was 0.82 V vs the reversible hydrogen electrode (RHE), and the average number of exchanged electrons, n, was equal to 3.87 as determined by RRDE. In the case of metallic catalysts, E_{onset} and n were in the range of 0.88−0.89 V and 3.85−3.98, respectively (details are given in the SI, Figure S2, and Table S2). First, the AEMFC performance of the MEA with the Pt-based cathode was evaluated, as shown in Figure S3, indicating adequate membrane efficiency in terms of cell polarization. Similarly, the PGM-free Ag (Figure S4) and $(MnCo)_3O_4$ (Figure S5) and ultralow PGM PdAg (Figure S6) cathode catalysts were evaluated in AEMFCs to corroborate the performance they displayed in the RRDE experiments.

Operando measurements were performed with an AEMFC inserted into a resonator of an EPR spectrometer, and the formation of radicals was monitored by the spin trapping technique using a DMPO spin trap, which bonds to short-living, reactive radicals forming a stable, detectable adduct. The operando experiments allow for the investigation of the reactions at the catalyst surface, the involvement of the radicals, and all species transport phenomena through the AEM, which are not possible in ex situ studies. Placing the spin trap directly onto the cathode allowed us to study radical formation on the cathode side.[18] These experiments (see SI, section Experimental Methods viii, p 10) evidenced that DMPO diffused across the FAA-3-20-rf AEM in 25 min as

https://doi.org/10.1021/acscatal.2c05843
ACS Catal. 2023, 13, 2744−2750

shown in Table S4, so we limited our observations to 15 min, regardless of the observed slow diffusion of DMPO. In this study, we investigated only the cathode side since oxygen radicals are most expected to attack the membrane[26,27] and carbon support, leading to their deterioration.[28] The experimental (black solid line) and simulated (green dashed line) EPR spectra recorded just after starting the AEMFC EPR operation and DMPO applied on cathode sides are given in Figure 1 for all of the investigated cathode catalysts. The EPR spectra of spin adducts exhibit hyperfine splitting (HFS) from ^{14}N (nuclear spin $I = 1$, splitting the signal into three lines) and two ^{1}H ($I = 1/2$, splitting the signal into two lines) nuclei, one present in the spin trap molecule (H_β) and the second one originated from hydroperoxyl radical (H_γ), Figure 2A. The

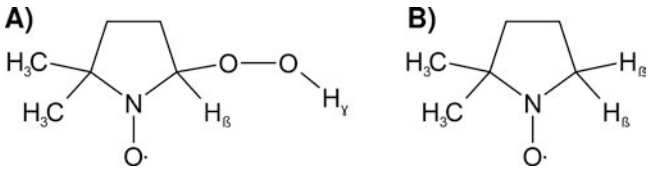

Figure 2. Structure of DMPO spin trap adducts with peroxide radicals (A) and hydrogen radicals (B).

scheme of the splitting for the DMPO-OOH adducts is presented in Figure S7A, and reference EPR spectra of the DMPO adducts formed in the AEMFC utilizing the FAA-3-20-rf membrane covered with the Pt catalyst are given in Figure S8.[18]

Registered spectra differ in signal-to-noise ratio; however, all spectra simulations revealed spectral parameters (collected in Table 1) typical for a •OOH radical adduct (Figure 2A).[18,29−31] To the best of our knowledge, this is the first time that radicals were measured and detected using different ORR catalysts in operando AEMFCs. Both PGM and PGM-free catalysts show the formation of a •OOH radical adduct,

Table 1. EPR Spectral Parameters of DMPO Adducts Detected during Experiments

		hyperfine splittings			
catalyst	adduct	A_N	$A_{H\beta}$	$A_{H\gamma}$	g
Pd (Figure 1A)	DMPO-OOH	13.1	11.1	2.4	2.0052
Ag (Figure 1B)	DMPO-OOH	13.7	11.4	1.1	2.0052
PdAg (Figure 1C)	DMPO-OOH	13.3	10.8	1.1	2.0061
$(MnCo)_3O_4$ (Figure 1D)	DMPO-OOH	13.7	11.4	0.91	2.0057
$(MnCo)_3O_4$ (Figure 3A)	DMPO-OOH	13.7	11.3	0.91	2.0058
$(MnCo)_3O_4$ (Figure 3B)	DMPO-OOH	13.6	11.3	0.91	2.0058
	DMPO-^{17}OOH	13.5	11.3	0.91	2.0058
				A_{17O} = 4.6	
PdAg (Figure 4A)	DMPO-OOH	12.8	11.7	2.4	2.0059
PdAg (Figure 4B)	DMPO-OOH	12.5	11.2	2.3	2.0061
	DMPO-H	14.6	20.3 ($H\beta_1$), 20.0 ($H\beta_2$)		2.0059
PdAg (Figure 5A)	DMPO-H	15.2	20.3 ($H\beta_1$), 20.3 ($H\beta_2$)		2.0057
Pt (Figure 5B)	DMPO-H	15.5	20.7 ($H\beta_1$), 20.7 ($H\beta_2$)		2.0054

which may suggest that in the alkaline medium of AEMFCs, radicals are always generated regardless of which ORR catalysts are used.

In a recent study, Meyerstein[32] suggests that many oxidizing agents might oxidize DMPO to form DMPO$^{\bullet+}$, which in aqueous media yields DMPO-OH.[33] To investigate if the DMPO-OOH adducts were detected due to spin trapping of the radicals formed on the catalyst surface, and not because of the DMPO oxidation by transition metals, additional experiments were performed employing the $(MnCo)_3O_4$ catalyst as a model system. After degassing the spinel sample in a vacuum at 300 °C, a DMPO spin trap was added. No EPR signals were present in the spectra of the evacuated spinel after the addition of DMPO (Figure S9). The signals appeared only after exposing the catalyst to oxygen at a pressure of 150 Torr. HFS constants and g-factor values indicate that the registered spectra originate from the DMPO-OOH adduct (Figure 3A). To further confirm the origin of •OOH radicals, a similar experiment was performed, this time using oxygen gas enriched

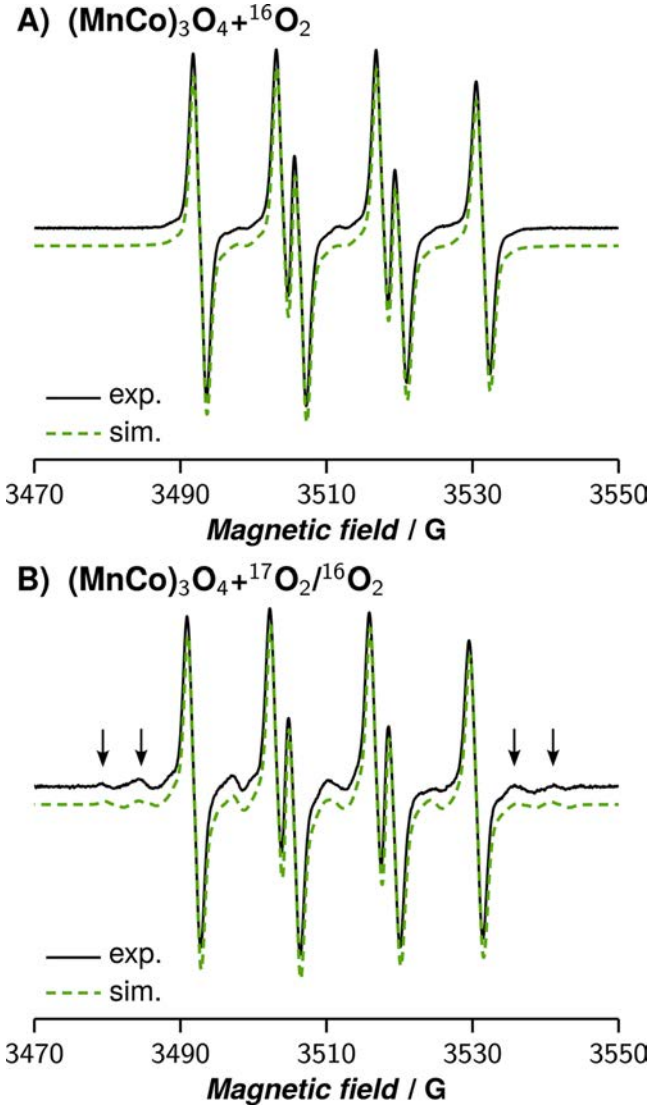

Figure 3. Experimental (black solid line) and simulated (green dashed line) EPR spectra of DMPO-OOH adducts formed while the $(MnCo)_3O_4$ catalyst was exposed to 150 Torr of $^{16}O_2$ (A) and 10 Torr of 70% $^{17}O_2$/30% $^{16}O_2$ (B).

https://doi.org/10.1021/acscatal.2c05843
ACS Catal. 2023, 13, 2744−2750

in an ^{17}O isotope. Registered spectra are shown in Figure 3B, exhibiting additional lines in comparison to the spectrum obtained with ^{16}O (Figure 3A). Extra signals are due to HFS coming from ^{17}O atoms with $I = 5/2$ and A_{17O} equal to 4.6 G, and the outermost lines are marked by the arrows. This result clearly indicates that the hydroperoxide radicals are generated from gaseous oxygen interacting with the catalyst and that the registered EPR signal is not due to spin trap oxidation by a metal redox pair.

The spectra recorded on the AEMFC cathode side at the start and after 15 min of operation are shown in Figure 4A,B.

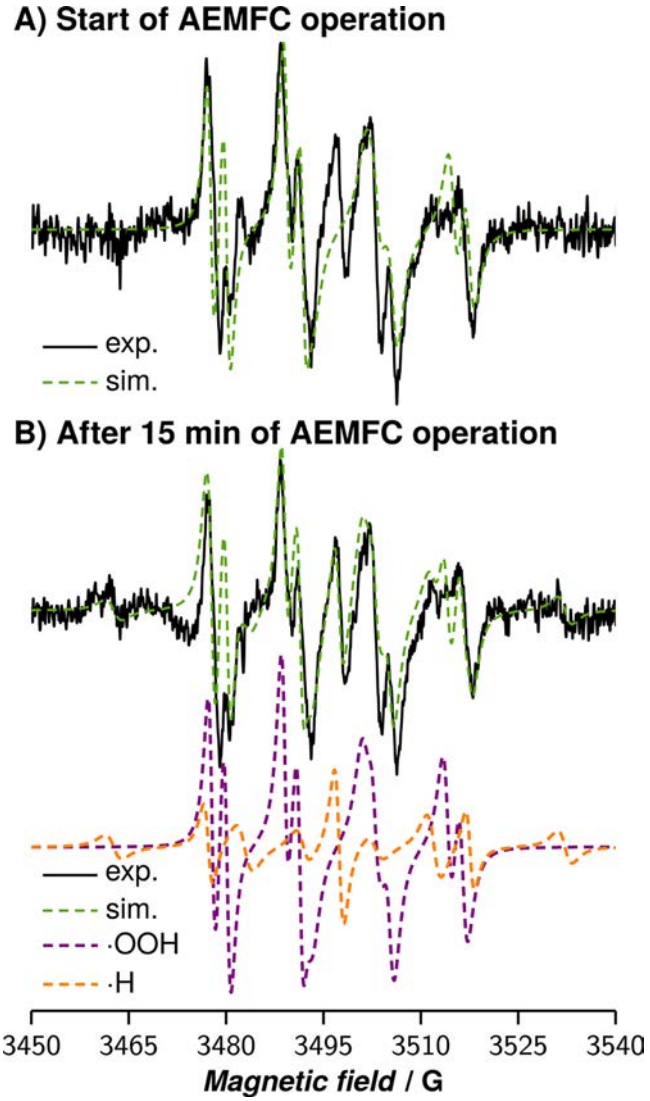

Figure 4. Experimental (black solid line) and simulated (green dashed line) EPR spectra of DMPO spin trap adducts recorded on the cathode side of the AEMFC using the PdAg alloy as a cathode catalyst at the beginning (A) and after 15 min of FC operation (B). Component spectra of B are marked as orange and violet lines.

After that time of CCV operation of the AEMFC employing the PdAg cathode catalyst, the gradual appearance of an EPR signal originating from the adduct of the DMPO trap with $^{\bullet}H$ radicals was observed. The signal is due to HFS induced by two hydrogen nuclei interacting with the unpaired electron (Figure 2B, the splitting scheme is given in Figure S7B). In Figure 4B, two component spectra are used for the simulation of the EPR spectrum. We postulate that the appearance of hydrogen radicals is due to the permeation of hydrogen through the AEM, followed by its subsequent activation on the cathode catalyst.[29]

To confirm these ideas, two sets of experiments were performed. First, the possibility of hydrogen activation to $^{\bullet}H$ radicals on PdAg was examined. The DMPO spin trap was placed on the catalyst layer and exposed directly to hydrogen flow in the AEMFC. In such a case, the typical EPR signal for DMPO-H adducts was observed, indicating that the PdAg catalyst can produce hydrogen radicals (Figure 5A). In the

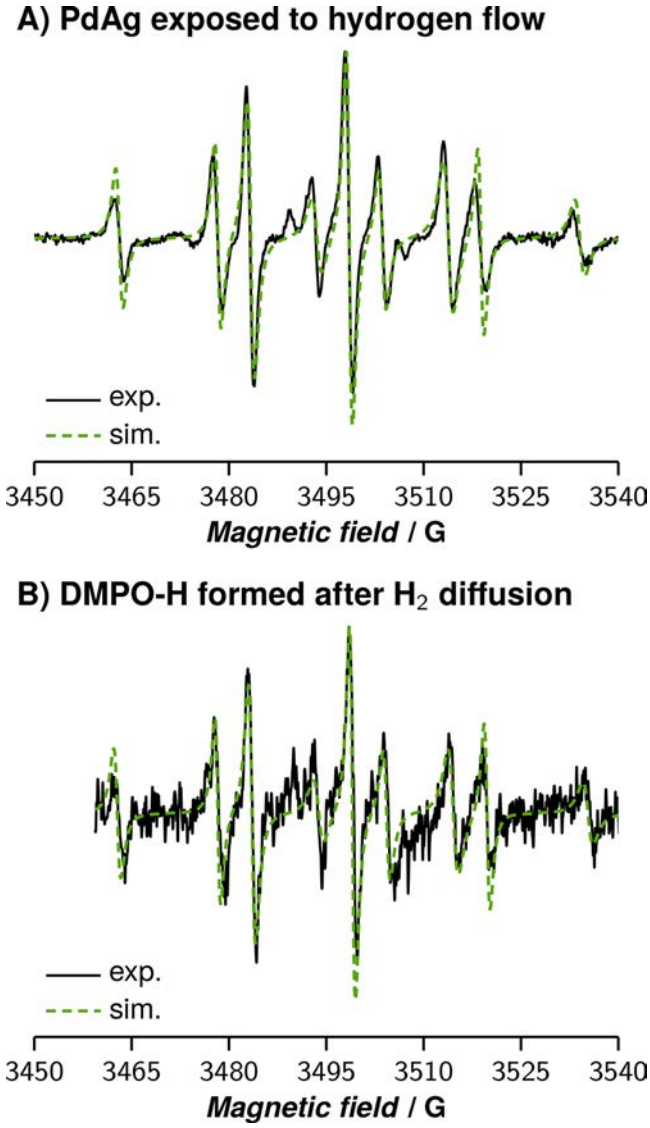

Figure 5. Experimental (black solid line) and simulated (green dashed line) EPR spectra of DMPO spin trap adducts recorded on the PdAg alloy exposed to hydrogen flow (A) and on the Pt covered with DMPO after diffusion of H_2 through the membrane (B).

second test, the membrane was covered with the platinum catalyst only on one side, and the spin trap was placed on the catalyst layer. Then, the hydrogen was applied on the side without Pt and DMPO. After 2−5 min, the EPR signal from DMPO-H adducts appeared. Since catalysts were not present on the hydrogen side, we conclude that the H_2 can diffuse through the membrane (Figure 5B and Table S4).

https://doi.org/10.1021/acscatal.2c05843
ACS Catal. 2023, 13, 2744−2750

Knowing that in the alkaline medium of AEMFCs we may expect •H and •OOH radicals to be formed at the cathode during the operation is crucial. The formation of these radicals during AEMFC operation may have significant implications for the understanding of cell degradation. While the mechanisms of AEM degradation by OH^- are well-established,[34] radical-induced degradation remains largely unknown. They are, however, suspected of playing a crucial role in the degradation of cationic moieties of the AEMs.[26,27]

Therefore, radical scavenging strategies to mitigate AEM degradation are a potential way to address this challenge.[35−37] We intend to address this issue in future studies by modifying the catalyst with radical scavenger materials and performing similar EPR measurements to examine the radical formation and comparing those without radical scavenger materials.[38] For example, for the cathode ORR, we plan to synthesize the $MnCoO_x$ catalyst with CeO_x, while the anode HOR catalyst will have TiO_x-decorated Pt and CeO_x-decorated Pd.

CONCLUSIONS

We have investigated the formation of radicals on different classes of platinum group metal (PGM) and PGM-free oxygen reduction reaction (ORR) catalysts in operando AEMFCs. The results presented in this study indicate that radicals are formed during cell operation regardless of the type of catalysts used, suggesting that the formation of the radicals during the alkaline ORR is a general phenomenon and does not depend on the catalysts' nature. Additionally, the experiment with ^{17}O enriched gas proved that •OOH radicals are created from the gaseous oxygen interacting with the spinel catalysts and not by oxidation of the spin trap by metal cations. It was also shown that hydrogen crossover can cause the formation of •H radicals at the AEMFC cathode. The formation of •H and •OOH radicals at the cathode during the AEMFC operation is crucial for the understanding of cell degradation. These findings suggest that it is necessary to develop new catalysts containing radical scavenging additives as well as novel anion-exchange membranes able to withstand radical attack. Thus, in our future studies, we plan to investigate the efficacy of radical scavenging materials such as CeO_x and TiO_x, as well as the effect of operating conditions on the formation of the radicals by varying the relative humidity, temperature, type of AEM, and catalyst supports.

ASSOCIATED CONTENT

Supporting Information

The Supporting Information is available free of charge at https://pubs.acs.org/doi/10.1021/acscatal.2c05843.

Materials, experimental methods; Figures S1−S9; Tables S1−S4; experimental data; XRD, FC, and RRDE data; additional EPR data; HFS schemes (PDF)

AUTHOR INFORMATION

Corresponding Authors

Dario R. Dekel − *The Wolfson Department of Chemical Engineering, Technion—Israel Institute of Technology, Haifa 3200003, Israel; The Nancy and Stephen Grand Technion Energy Program (GTEP), Technion—Israel Institute of Technology, Haifa 3200003, Israel;* orcid.org/0000-0002-8610-0808; Email: dario@technion.ac.il

Krzysztof Kruczała − *Faculty of Chemistry, Jagiellonian University in Krakow, 30-387 Krakow, Poland;* orcid.org/0000-0002-1241-6789; Email: kruczala@chemia.uj.edu.pl

Authors

Szymon Wierzbicki − *Faculty of Chemistry, Jagiellonian University in Krakow, 30-387 Krakow, Poland; Doctoral School of Exact and Natural Sciences, Jagiellonian University in Krakow, 30-387 Krakow, Poland;* orcid.org/0000-0002-3533-5885

John C. Douglin − *The Wolfson Department of Chemical Engineering, Technion—Israel Institute of Technology, Haifa 3200003, Israel;* orcid.org/0000-0003-4151-1424

Ramesh K. Singh − *The Wolfson Department of Chemical Engineering, Technion—Israel Institute of Technology, Haifa 3200003, Israel; CO_2 Research and Green Technologies Centre, Vellore Institute of Technology (VIT), Vellore 632014 Tamil Nadu, India*

Complete contact information is available at: https://pubs.acs.org/10.1021/acscatal.2c05843

Author Contributions

The manuscript was written through the contributions of all authors. All authors have approved the final version of the manuscript.

Notes

The authors declare no competing financial interest.

ACKNOWLEDGMENTS

This work was supported by the Polish National Science Centre under grant no. 2017/27/B/ST5/01004, by the Nancy and Stephen Grand Technion Energy Program (GTEP), and by the Israeli Science Foundation (ISF), grant number 169/22. S.W. is grateful to the program "Excellence Initiative − Research University" at Jagiellonian University. J.C.D. thanks Dr. Irwin and Mrs. Joan Jacobs for their generous financial support in the form of the Jacobs Excellence Scholarship. J.C.D. also thanks The Israeli Smart Transportation Research Center for their generous financial support in the form of the ISTRC Scholarship.

REFERENCES

(1) Yang, Y.; Peltier, C. R.; Zeng, R.; Schimmenti, R.; Li, Q.; Huang, X.; Yan, Z.; Potsi, G.; Selhorst, R.; Lu, X.; Xu, W.; Tader, M.; Soudackov, A. V.; Zhang, H.; Krumov, M.; Murray, E.; Xu, P.; Hitt, J.; Xu, L.; Ko, H.-Y.; Ernst, B. G.; Bundschu, C.; Luo, A.; Markovich, D.; Hu, M.; He, C.; Wang, H.; Fang, J.; DiStasio, R. A.; Kourkoutis, L. F.; Singer, A.; Noonan, K. J. T.; Xiao, L.; Zhuang, L.; Pivovar, B. S.; Zelenay, P.; Herrero, E.; Feliu, J. M.; Suntivich, J.; Giannelis, E. P.; Hammes-Schiffer, S.; Arias, T.; Mavrikakis, M.; Mallouk, T. E.; Brock, J. D.; Muller, D. A.; DiSalvo, F. J.; Coates, G. W.; Abruña, H. D. Electrocatalysis in Alkaline Media and Alkaline Membrane-Based Energy Technologies. *Chem. Rev.* **2022**, *122* (6), 6117−6231.

(2) Dekel, D. R. Review of Cell Performance in Anion Exchange Membrane Fuel Cells. *J. Power Sources* **2018**, *375*, 158−169.

(3) Gottesfeld, S.; Dekel, D. R.; Page, M.; Bae, C.; Yan, Y.; Zelenay, P.; Kim, Y. S. Anion Exchange Membrane Fuel Cells: Current Status and Remaining Challenges. *J. Power Sources* **2018**, *375*, 170−184.

(4) Huang, G.; Mandal, M.; Peng, X.; Yang-Neyerlin, A. C.; Pivovar, B. S.; Mustain, W. E.; Kohl, P. A. Composite Poly(Norbornene) Anion Conducting Membranes for Achieving Durability, Water Management and High Power (3.4 W/cm²) in Hydrogen/Oxygen Alkaline Fuel Cells. *J. Electrochem. Soc.* **2019**, *166* (10), F637−F644.

(5) Omasta, T. J.; Park, A. M.; LaManna, J. M.; Zhang, Y.; Peng, X.; Wang, L.; Jacobson, D. L.; Varcoe, J. R.; Hussey, D. S.; Pivovar, B. S.; Mustain, W. E. Beyond Catalysis and Membranes: Visualizing and

Solving the Challenge of Electrode Water Accumulation and Flooding in AEMFCs. *Energy Environ. Sci.* **2018**, *11* (3), 551−558.
(6) Omasta, T. J.; Peng, X.; Miller, H. A.; Vizza, F.; Wang, L.; Varcoe, J. R.; Dekel, D. R.; Mustain, W. E. Beyond 1.0 W Cm^{-2} Performance without Platinum: The Beginning of a New Era in Anion Exchange Membrane Fuel Cells. *J. Electrochem. Soc.* **2018**, *165* (15), J3039−J3044.
(7) Douglin, J. C.; Singh, R. K.; Hamo, E. R.; Hassine, M. B.; Ferreira, P. J.; Rosen, B. A.; Miller, H. A.; Rothenberg, G.; Dekel, D. R. Performance Optimization of PGM and PGM-Free Catalysts in Anion-Exchange Membrane Fuel Cells. *J. Solid State Electrochem* **2022**, *26* (9), 2049−2057.
(8) Ni, W.; Wang, T.; Héroguel, F.; Krammer, A.; Lee, S.; Yao, L.; Schüler, A.; Luterbacher, J. S.; Yan, Y.; Hu, X. An Efficient Nickel Hydrogen Oxidation Catalyst for Hydroxide Exchange Membrane Fuel Cells. *Nat. Mater.* **2022**, *21* (7), 804−810.
(9) Zion, N.; Douglin, J. C.; Cullen, D. A.; Zelenay, P.; Dekel, D. R.; Elbaz, L. Porphyrin Aerogel Catalysts for Oxygen Reduction Reaction in Anion-Exchange Membrane Fuel Cells. *Adv. Funct Mater.* **2021**, *31* (24), 2100963.
(10) Zhu, W.; Pei, Y.; Douglin, J. C.; Zhang, J.; Zhao, H.; Xue, J.; Wang, Q.; Li, R.; Qin, Y.; Yin, Y.; Dekel, D. R.; Guiver, M. D. Multi-Scale Study on Bifunctional Co/Fe−N−C Cathode Catalyst Layers with High Active Site Density for the Oxygen Reduction Reaction. *Appl. Catal., B* **2021**, *299*, 120656.
(11) Kostuch, A.; Gryboś, J.; Wierzbicki, S.; Sojka, Z.; Kruczała, K. Selectivity of Mixed Iron-Cobalt Spinels Deposited on a N,S-Doped Mesoporous Carbon Support in the Oxygen Reduction Reaction in Alkaline Media. *Materials* **2021**, *14* (4), 820.
(12) Kostuch, A.; Jarczewski, S.; Surówka, M. K.; Kuśtrowski, P.; Sojka, Z.; Kruczała, K. The Joint Effect of Electrical Conductivity and Surface Oxygen Functionalities of Carbon Supports on the Oxygen Reduction Reaction Studied over Bare Supports and Mn−Co Spinel/Carbon Catalysts in Alkaline Media. *Catal. Sci. Technol.* **2021**, *11* (23), 7578−7591.
(13) Kostuch, A.; Gryboś, J.; Indyka, P.; Osmieri, L.; Specchia, S.; Sojka, Z.; Kruczała, K. Morphology and Dispersion of Nanostructured Manganese-Cobalt Spinel on Various Carbon Supports: The Effect on the Oxygen Reduction Reaction in Alkaline Media. *Catal. Sci. Technol.* **2018**, *8* (2), 642−655.
(14) Mustain, W. E.; Chatenet, M.; Page, M.; Kim, Y. S. Durability Challenges of Anion Exchange Membrane Fuel Cells. *Energy Environ. Sci.* **2020**, *13* (9), 2805−2838.
(15) Biemolt, J.; Douglin, J. C.; Singh, R. K.; Davydova, E. S.; Yan, N.; Rothenberg, G.; Dekel, D. R. An Anion-Exchange Membrane Fuel Cell Containing Only Abundant and Affordable Materials. *Energy Technology* **2021**, *9* (4), 2000909.
(16) Yang-Neyerlin, A. C.; Medina, S.; Meek, K. M.; Strasser, D. J.; He, C.; Knauss, D. M.; Mustain, W. E.; Pylypenko, S.; Pivovar, B. S. Eds.' Choice—Examining Performance and Durability of Anion Exchange Membrane Fuel Cells with Novel Spirocyclic Anion Exchange. *Membranes. J. Electrochem Soc.* **2021**, *168* (4), 044525.
(17) Gao, F.-Y.; Liu, S.-N.; Ge, J.-C.; Zhang, X.-L.; Zhu, L.; Zheng, Y.-R.; Duan, Y.; Qin, S.; Dong, W.; Yu, X.; Bao, R.-C.; Yang, P.-P.; Niu, Z.-Z.; Ding, Z.-G.; Liu, W.; Lan, S.; Gao, M.-R.; Yan, Y.; Yu, S.-H. Nickel−Molybdenum−Niobium Metallic Glass for Efficient Hydrogen Oxidation in Hydroxide Exchange Membrane Fuel Cells. *Nat. Catal* **2022**, *5* (11), 993−1005.
(18) Wierzbicki, S.; Douglin, J. C.; Kostuch, A.; Dekel, D. R.; Kruczała, K. Are Radicals Formed during Anion-Exchange Membrane Fuel Cell Operation? *J. Phys. Chem. Lett.* **2020**, *11* (18), 7630−7636.
(19) Wang, L.; Brink, J. J.; Varcoe, J. R. The First Anion-Exchange Membrane Fuel Cell to Exceed 1 W cm^{-2} at 70°C with a Non-Pt-Group (O2) Cathode. *Chem. Commun.* **2017**, *53* (86), 11771−11773.
(20) Zamora Zeledón, J. A.; Stevens, M. B.; Gunasooriya, G. T. K. K.; Gallo, A.; Landers, A. T.; Kreider, M. E.; Hahn, C.; Nørskov, J. K.; Jaramillo, T. F. Tuning the Electronic Structure of Ag-Pd Alloys to Enhance Performance for Alkaline Oxygen Reduction. *Nat. Commun.* **2021**, *12* (1), 620.
(21) Yang, Y.; Peng, H.; Xiong, Y.; Li, Q.; Lu, J.; Xiao, L.; DiSalvo, F. J.; Zhuang, L.; Abruña, H. D. High-Loading Composition-Tolerant Co−Mn Spinel Oxides with Performance beyond 1 W/cm^2 in Alkaline Polymer Electrolyte Fuel Cells. *ACS Energy Lett.* **2019**, *4* (6), 1251−1257.
(22) Li, K.; Zhang, R.; Gao, R.; Shen, G.-Q.; Pan, L.; Yao, Y.; Yu, K.; Zhang, X.; Zou, J.-J. Metal-Defected Spinel $Mn_xCo_{3-x}O_4$ with Octahedral Mn-Enriched Surface for Highly Efficient Oxygen Reduction Reaction. *Appl. Catal., B* **2019**, *244*, 536−545.
(23) Spałek, T.; Pietrzyk, P.; Sojka, Z. Application of the Genetic Algorithm Joint with the Powell Method to Nonlinear Least-Squares Fitting of Powder EPR Spectra. *J. Chem. Inf Model* **2005**, *45* (1), 18−29.
(24) Panchenko, A.; Dilger, H.; Möller, E.; Sixt, T.; Roduner, E. In Situ EPR Investigation of Polymer Electrolyte Membrane Degradation in Fuel Cell Applications. *J. Power Sources* **2004**, *127* (1−2), 325−330.
(25) Ross, J. R. H. Catalyst Characterization. In *Contemporary Catalysis*; Elsevier, 2019; 121−132.
(26) Nemeth, T.; Nauser, T.; Gubler, L. On the Radical-Induced Degradation of Quaternary Ammonium Cations for Anion-Exchange Membrane Fuel Cells and Electrolyzers. *ChemSusChem* **2022**, *15* (22), e202201571.
(27) Zhang, Y.; Parrondo, J.; Sankarasubramanian, S.; Ramani, V. Detection of Reactive Oxygen Species in Anion Exchange Membrane Fuel Cells Using In Situ Fluorescence Spectroscopy. *ChemSusChem* **2017**, *10* (15), 3056−3062.
(28) Singh, H.; Zhuang, S.; Ingis, B.; Nunna, B. B.; Lee, E. S. Carbon-Based Catalysts for Oxygen Reduction Reaction: A Review on Degradation Mechanisms. *Carbon N Y* **2019**, *151*, 160−174.
(29) Łańcucki, L.; Schlick, S.; Danilczuk, M.; Coms, F. D.; Kruczała, K. Sulfonated Poly(Benzoyl Paraphenylene) as a Membrane for PEMFC: Ex Situ and in Situ Experiments of Thermal and Chemical Stability. *Polym. Degrad. Stab.* **2013**, *98* (1), 3−11.
(30) Danilczuk, M.; Coms, F. D.; Schlick, S. Visualizing Chemical Reactions and Crossover Processes in a Fuel Cell Inserted in the Esr Resonator: Detection by Spin Trapping of Oxygen Radicals, Nafion-Derived Fragments, and Hydrogen and Deuterium Atoms. *J. Phys. Chem. B* **2009**, *113* (23), 8031−8042.
(31) Danilczuk, M.; Schlick, S.; Coms, F. D. Detection of Radicals by Spin Trapping ESR in a Fuel Cell Operating with a Sulfonated Poly(Ether Ether Ketone) (SPEEK) Membrane. *Macromolecules* **2013**, *46* (15), 6110−6117.
(32) Meyerstein, D. Re-Examining Fenton and Fenton-like Reactions. *Nat. Rev. Chem.* **2021**, *5* (9), 595−597.
(33) Eberson, L.; Balinov, B.; Hagelin, G.; Dugstad, H.; Thomassen, T.; Forngren, B. H.; Forngren, T.; Hartvig, P.; Markides, K.; Yngve, U.; Ögren, M. Formation of Hydroxyl Spin Adducts via Nucleophilic Addition−Oxidation to 5,5-Dimethyl-1-Pyrroline N-Oxide (DMPO). *Acta Chem. Scand.* **1999**, *53*, 584−593.
(34) Chatenet, M.; Pollet, B. G.; Dekel, D. R.; Dionigi, F.; Deseure, J.; Millet, P.; Braatz, R. D.; Bazant, M. Z.; Eikerling, M.; Staffell, I.; Balcombe, P.; Shao-Horn, Y.; Schäfer, H. Water Electrolysis: From Textbook Knowledge to the Latest Scientific Strategies and Industrial Developments. *Chem. Soc. Rev.* **2022**, *51* (11), 4583−4762.
(35) Trogadas, P.; Parrondo, J.; Ramani, V. CeO_2 Surface Oxygen Vacancy Concentration Governs in Situ Free Radical Scavenging Efficacy in Polymer Electrolytes. *ACS Appl. Mater. Interfaces* **2012**, *4* (10), 5098−5102.
(36) Xie, H.; Xie, X.; Hu, G.; Prabhakaran, V.; Saha, S.; Gonzalez-Lopez, L.; Phakatkar, A. H.; Hong, M.; Wu, M.; Shahbazian-Yassar, R.; Ramani, V.; Al-Sheikhly, M. I.; Jiang, D.; Shao, Y.; Hu, L. Ta−TiO_x Nanoparticles as Radical Scavengers to Improve the Durability of Fe−N−C Oxygen Reduction Catalysts. *Nat. Energy* **2022**, *7* (3), 281−289.
(37) Prabhakaran, V.; Arges, C. G.; Ramani, V. Investigation of Polymer Electrolyte Membrane Chemical Degradation and Degradation Mitigation Using in Situ Fluorescence Spectroscopy. *Proc. Natl. Acad. Sci. U. S. A.* **2012**, *109* (4), 1029−1034.

https://doi.org/10.1021/acscatal.2c05843
ACS Catal. 2023, 13, 2744−2750

(38) Kruczała, K.; Szczubiałka, K.; Łańcucki, Ł.; Zastawny, I.; Góra-Marek, K.; Dyrek, K.; Sojka, Z. Spectroscopic Investigations into Degradation of Polymer Membranes for Fuel Cells Applications. *Spectrochim Acta A Mol. Biomol Spectrosc* **2008**, *69* (5), 1337−1343.

https://doi.org/10.1021/acscatal.2c05843
ACS Catal. 2023, 13, 2744−2750